Combining amoxicillin and relebactam provides a new therapeutic option for *Mycobacterium abscessus* infection

Rose C. Lopeman[1†], James Harrison[1†], Savannah E. R. Gibson[1], Daniel L. Rathbone[1], Maya Desai[2], Peter Lambert[1] and Jonathan A. G. Cox[1]*

[1]School of Life and Health Sciences, Aston University, Aston Triangle, Birmingham, UK, B4 7ET

[2]Birmingham Children's Hospital, Birmingham Women's and Children's NHS Foundation Trust, Steelhouse Lane, Birmingham, UK, B4 6NH

[†]These authors contributed equally to this work.

*Author to whom correspondence should be addressed:

Dr Jonathan A. G. Cox, School of Life and Health Sciences, Aston University, Aston Triangle, Birmingham, UK, B4 7ET; J.a.g.cox@aston.ac.uk; 0(+44)121 204 5011

ORCID ID: 0000-0001-5208-4056

Key Words:

Mycobacterium abscessus; Non-tuberculous mycobacteria; Antimicrobial drug discovery; Cystic fibrosis; β-lactam; β-lactamase; synergy

Abstract:

Infections caused by the opportunistic pathogen *Mycobacterium abscessus* are increasing in prevalence within the cystic fibrosis population. Our limited understanding of this ubiquitous environmental microorganism matched with its intrinsic resistance to most classes of antibiotic, including β-lactams, has left us with an urgent demand for new, more effective therapeutic interventions. *De novo* antimicrobial drug discovery is a lengthy process and so we have taken the approach of repurposing known antibiotics in order to provide a rapidly implementable solution to a current problem. Here we report a significant potential step forward in the treatment of *M. abscessus* infection by sensitising the organism to the broad spectrum β-lactam antibiotic, amoxicillin, using the competitive β-lactamase inhibitor, relebactam. We demonstrate by disk diffusion and broth microdilution assay that this combination works synergistically to inhibit *M. abscessus.* We also demonstrate the direct competitive inhibition of the *M. abscessus* β-lactamase, Bla_{Mab}, using a novel thin-layer chromatography-based assay for β-lactamase inhibition, which is subsequently validated kinetically by spectrophotometric assay using the nitrocefin reporter assay and *in silico* binding studies. Furthermore, we reverse the sensitivity by overexpressing Bla_{Mab} in *M. abscessus*, demonstrating relebactam-Bla_{Mab} target engagement. Finally, we demonstrate the *in vitro* efficacy of this combination against a collection of *M. abscessus* clinical isolates, as well as the *Mycobacterium tuberculosis* model organism *Mycobacterium bovis* BCG, demonstrating the significant therapeutic potential of the amoxicillin and relebactam combination.

Introduction:

The incidence of infections with the rapidly growing non-tuberculous mycobacterial (NTM) organism *Mycobacterium abscessus* is increasing due to the increase of immunocompromised individuals (Petrini, et al. 2006) (Griffith, et al. 2014). *M. abscessus* is widely responsible for opportunistic pulmonary infections in patients with structural lung disorders such as cystic fibrosis (CF) and

47 bronchiectasis (Griffith, et al., 2007) as well as skin and soft tissue infections (SSTIs) in humans
48 (Moore, 1953) (Fitzgerald, et al., 1995). The ubiquitous environmental nature of *M. abscessus* may
49 go some way to explaining the high levels of intrinsic drug resistance to most major classes of
50 antibiotic that is observed clinically (Nessar, et al. 2012). Recently, macrolides were added to the
51 ever growing list of ineffective antimicrobial agents for *M. abscessus* infection, exemplifying the
52 urgent need for new ways to treat this infection (Nessar, et al. 2012). Additionally, *M. abscessus* is
53 resistant to two of the frontline antibiotics used for tuberculosis treatment; rifampicin and
54 ethambutol (Nessar, et al. 2012), and many of the new drugs being discovered for treating
55 tuberculosis do not exhibit any antimicrobial activity against *M. abscessus* (Soni, et al. 2016).

56

57 Pulmonary *M. abscessus* disease was historically treated with macrolide antibiotics such as
58 clarithromycin (Griffith, et al., 2007), however the steady emergence of antibiotic resistant strains
59 has prompted the implementation of combination therapy using azithromycin (macrolide) along
60 with amikacin (aminoglycoside) and at least one other drug of a different class (Leung, et al. 2013).
61 The British Thoracic Society recommends a biphasic treatment for pulmonary *M. abscessus* infection
62 comprising of a 1-month initiation phase including intravenously administered amikacin, tigecycline
63 and imipenem, supplemented with oral clarithromycin or azithromycin (depending on sensitivity
64 results). This is followed by a 12-month continuation phase comprising of nebulised amikacin, and a
65 combination of 1-4 of clofazimine, linezolid, minocycline, moxifloxacin or co-trimoxaole (Lopeman et
66 al. 2019) (Haworth et al 2017).

67

68 The advancements in whole genome sequencing technology have enabled the identification of three
69 distinct subspecies within the *M. abscessus* complex, comprising *M. abscessus* subsp. *abscessus, M.*
70 *abscessus* subsp. *bolletii,* and *M. abscessus* subsp. *massiliense,* the latter of which contains a non-
71 functional *erm*(41) gene, resulting in a macrolide sensitive phenotype (Bryant et al. 2013) (Tortoli et

72 al. 2016). Mutations in *rrs* and *rrl* 16S rRNA genes have been identified corresponding to high levels
73 of aminoglycoside resistance, prohibiting the effective use of amikacin in treatment for *M. abscessus*
74 subsp. a*bscessus* and *M. abscessus* subsp. m*assiliense* clinical isolates specifically (Kehrmann et al.
75 2016). All *M. abscessus* subsp. contain an endogenous class A β-lactamase (Bla_{Mab}) conveying
76 intrinsic resistance to the β-lactam antibiotics (Soroka et al 2014). The identification of Bla_{Mab}, a
77 homolog of the *Mycobacterium tuberculosis* endogenous β-lactamase, BlaC, sparked widespread
78 investigation into the potential of β-lactamase inhibitors to supplement the treatment of *M.*
79 *abscessus* infection. A study demonstrated the inhibitory activity of avibactam, a non-β-lactam β-
80 lactamase inhibitor, against Bla_{Mab} significantly improving the *in vitro* and *in vivo* activity of
81 imipenem (Lefebvre et al. 2016). Recently, multiple studies have been published demonstrating a
82 number of β-lactam combinations displaying high levels of *in vitro* synergistic activity against *M.*
83 *abscessus* complex (Pandey et al 2019) (Story-Roller et al. 2019). Furthermore, one of these studies
84 identified the *in vitro* activity of two new non-β-lactam β-lactamase inhibitors, namely relebactam
85 and vaborbactam, demonstrating synergistic activity between imipenem and relebactam as well as
86 meropenem and vaborbactam (Kaushik et al. 2019).

87

88 In this study, we have built on previous work (Kaushik *et al.* 2019) and identified a significant step
89 forward in treatment potential for *M. abscessus* infection. We demonstrate the *in vitro* capacity for
90 sensitising the organism to the broad spectrum β-lactam antibiotic, amoxicillin, using the β-
91 lactamase inhibitor, relebactam. We establish synergy between amoxicillin and relebactam as well
92 as activity against a range of *M. abscessus* clinical isolates. We have identified the mechanism of
93 relebactam-Bla_{Mab} inhibition as competitive using recombinant protein in both a novel thin-layer
94 chromatography (TLC)-based assay, as well as previously established spectrophotometric methods.
95 Furthermore, this has been delineated using *in silico* molecular docking. This offers a considerable
96 therapeutic potential as imipenem, a mainstay of current *M. abscessus* treatment, is currently

97 undergoing phase III clinical trials in combination with relebactam, suggesting the simple addition of
98 amoxicillin and relebactam to the treatment regime has the potential to significantly improve the
99 treatment outcome.

100

101 **Materials and Methods:**

102 **Bacterial isolates**

103 A total of 16 *M. abscessus* clinical isolates from Brighton and Sussex Medical School and *M.*
104 *abscessus* NCTC 13031 were used in this study, along with *Mycobacterium bovis* BCG Pasteur. Stock
105 solutions of the isolates were kept in 50% glycerol (Sigma, Dorset, UK) and Middlebrook 7H9 Broth
106 and stored at -80 °C. Isolates were grown in Middlebrook 7H9 medium supplemented with 10% oleic
107 acid-dextrose-catalase (OADC), 1% glycerol (50% w/v) and 0.05% Tween 80 (v/v) prior to testing.
108 *Escherichia coli* Top 10 cells were used for propagation of plasmid DNA. These cells were routinely
109 grown in nutrient broth, or nutrient agar (Oxoid, UK) at 37 °C. *E. coli* BL21 (DE3) cells were used for
110 the overproduction of recombinant protein, grown in Terrific Broth (Melford, UK) at 37 °C.

111

112 **Antimicrobials**

113 The antimicrobial agents meropenem (MEM), amoxicillin (AMX) and phenoxymethylpenicillin
114 (Penicillin V/PenV) were obtained from Sigma Aldrich (Dorset, UK) and relebactam (REL) was
115 obtained from Carbosynth (Compton, UK). Stock solutions were prepared in sterile de-ionised water
116 and stored at -20 °C until use.

117

118 **Disk diffusions**

119 For the disk diffusion assays, *M. abscessus* clinical isolates were grown in Middlebrook 7H9 Broth to
120 logarithmic phase and 100 µL of bacterial culture was inoculated into 10 mL Middlebrook 7H9 Broth
121 supplemented with 0.7% bacteriological agar. This was poured as a layer in agar plates on top of 15
122 mL Middlebrook 7H11 Agar supplemented with 10% OADC and 1% glycerol. 6 mm sterile filter paper
123 diffusion disks were placed on the agar and were subsequently impregnated with antibiotic at the
124 following concentrations in sterile distilled water: relebactam 1 µL of 10 mg/mL, amoxicillin 3.3 µL of
125 3 mg/mL and meropenem 1 µL of 10 mg/mL. Plates were incubated at 30 °C for 5 days or until clear
126 zones of inhibition were visualised. Zones of inhibition were measured across the diameter to
127 include the disk itself. Disk diffusions were also performed on *M. abscessus* pVV16-bla_{Mab} and *M.*
128 *abscessus* pVV16.

129

130 **Broth microdilution assay**

131 The broth microdilution assay was performed as described previously with alterations appropriate to
132 this study (Institute, Clinican and Laboratory Standards 2012) (Caleffi-Ferracioli et al. 2013). Plates
133 were prepared by serially diluting amoxicillin (0.128 mg/mL – 0 mg/mL) or meropenem (0.128
134 mg/mL – 0 mg/mL) in the *x*-axis and relebactam (0.128 mg/mL – 0 mg/mL) in the *y*-axis. 80 µL of
135 *Mycobacterium abscessus* NCTC 13031 or *Mycobacterium bovis* BCG suspension adjusted to an
136 OD_{600} of 0.1-0.2 was inoculated in each well to reach a final well volume of 100 µL. Plates were
137 sealed and incubated at 30 °C for 5 days for *M. abscessus* cultures or 37 °C for 10 days for *M. bovis*
138 BCG. The MIC of amoxicillin/relebactam combination was determined by optical density
139 measurement using a spectrophotometric plate reader and identified as the well that had the lowest
140 concentrations of both compounds and exhibited no bacterial growth. The relevant well was
141 retroactively plotted into a growth curve over time, and this growth curve was compared to the
142 wells containing no drug, and the wells containing relebactam only and amoxicillin only. The broth
143 microdilution assay was also performed on *M. abscessus* pVV16-bla_{Mab} and *M. abscessus* pVV16.

144

145 **Generation of *M. abscessus* pVV16-*bla*$_{Mab}$ overexpressor strain**

146 The *bla*$_{Mab}$ gene (MAB_2875) from *Mycobacterium abscessus* NCTC 13031 was amplified by
147 polymerase chain reaction (PCR). Primers used were as follows (with restriction site underlined):
148 Forward primer AAAAAAGGATCCGCGCCGGACGAACTCGCC and Reverse primer
149 AAAAAAAAGCTTAGCGCCGAAGGCCCGCAG (Eurofins Genomics). Amplicons were purified and cloned
150 into pVV16 using *Bam*HI/*Hin*DIII restriction sites and the sequence was confirmed (Eurofins
151 Genomics). Both the plasmid pVV16 and the construct pVV16-*bla*$_{Mab}$ were inserted into *M. abscessus*
152 NCTC 13031 cells by electroporation (2.5kV, 2.5 µF and 1000 Ω).

153

154 **Expression and purification of recombinant Bla$_{Mab}$**

155 The *bla*$_{Mab}$ gene, with the first 90 base pairs omitted (resulting in a -30 residue N-terminal truncated
156 protein), was amplified by PCR using the following primers (with restriction sites underlined):
157 Forward primer AAAAAAGGATCCGCGCCGGACGAACTCGCC and Reverse primer
158 AAAAAAAAGCTTTCAAGCGCCGAAGGCCCG (Eurofins Genomics). Amplicons were purified and cloned
159 into pET28a using *Bam*HI/*Hin*DIII restriction sites and the sequence was confirmed (Eurofins
160 Genomics). Bla$_{Mab}$ was expressed in *E. coli* BL21 (DE3) cells by addition of 1 mM Isopropyl β-D-1-
161 thiogalactopyranoside (IPTG) and incubation at 25 °C for 18 h. Bla$_{Mab}$ was purified by Immobilised
162 Metal Affinity Chromatography (IMAC) and dialysed into 25 mM Tris HCl pH 7, 100 mM NaCl.

163

164 **Thin Layer Chromatography (TLC) activity assay**

165 Relebactam (2 mg/mL) was added to recombinant Bla$_{Mab}$ (0.01 mg/mL) and incubated for 5 minutes
166 at room temperature, before addition of Penicillin V (4 mg/mL) for a further 10 minute incubation at
167 room temperature. Alongside appropriate control reactions (Figure 2), 1 µL of the reaction was

168 spotted onto aluminium backed silica gel plates (5735 silica gel 60 F_{254}, Merck) and dried before
169 being subjected to Thin Layer Chromatography (TLC) using ethyl acetate:water:acetic acid
170 ($C_4H_8O_2$:H_2O:CH_3COOH) (3:1:1, v/v/v). Once dry, plates were visualised by being dipped into $KMnO_4$
171 TLC stain with light charring.

172

173 **Biochemical analysis of Bla_{Mab} inhibition by Relebactam**

174 Recombinant Bla_{Mab} (0.25 nM) was mixed with an increasing concentration of relebactam (0, 0.1, 1,
175 10 and 100 µM) and 100 µM nitrocefin (Carbosynth, UK). The hydrolysis of nitrocefin was monitored
176 at 486 nm using a Multiskan Go plate reader (Thermo Scientific). This was repeated using a varying
177 concentration of nitrocefin (1-500 µM) with a shorter range of relebactam concentrations (0, 0.5,
178 0.75, 1 and 2.5 µM) and initial velocities (v_i) were plotted against substrate concentration. Data
179 analysis was performed as previously described (Dubée et al., 2014, Papp-wallace et al., 2018). Data
180 analysis was conducted using Graphpad Prism 7.

181

182 The decarbamylation rate was determined by incubation of Bla_{Mab} (1 µM) with relebactam (20 µM)
183 for 1 hour at 25 °C. The reaction mixture was then subsequently diluted both 10,000 and 50,000 fold
184 (1.8 nM and 0.36 nM relebactam with 90 pM and 18 pM Bla_{Mab} respectively), before addition of 100
185 µM nitrocefin. The reaction was monitored at 486 nm using a Multiskan Go plate reader (Thermo
186 Scientific).

187

188 ***In Silico* Modelling of the Possible Interaction of Relebactam with the Bla_{Mab}**

189 The Bla_{Mab} X-ray crystal structure was obtained from the Protein Data Bank, accession code 4YFM.
190 The A chain was submitted to the GHECOM pocket-finding server (GHECOM 1.0) (Kawabata 2010;
191 Kawabata and Go 2007). The top six pockets identified were used to define the target site for

192 protein-ligand docking experiments between the enzyme and relebactam using CACHe Worksystem
193 Pro (version 7.5.0.85, Fujitsu Ltd). The amino acid residues lining theses pockets are given in Figure
194 3(c). Pocket 1 corresponded to the main (catalytic) site in the enzyme and for the purposes of the
195 docking experiment was redefined as all amino acid residues within 8 Å of serine 71. Hydrogen
196 atoms were added using the default settings in line with presumed protonation states for ionisable
197 amino acid side-chains. The positions of the added hydrogen atoms were optimised by locking the
198 coordinates of all the non-hydrogen atoms and subjecting the system to a molecular mechanics
199 (MM2) geometry optimisation. Relebactam was docked four times into each pocket, using CACHe
200 Worksystem Pro. The amino acid side-chains in each pocket were allowed to be flexible as were all
201 rotatable bonds in relebactam. The genetic algorithm settings for the docking protocol included
202 population size 50, maximum generations 3000, crossover rate 0.8, mutation Rate 0.2 and
203 convergence when the RMSD population fitness was less than 1. The best-scoring consensus
204 complexes from each series of dockings were taken forward for molecular dynamics simulation. The
205 required input files were prepared using the Antechamber module of the AMBER Tools package
206 (Version 14; Case et al, 2005), implementing the ff14SB force field. The system was neutralised by
207 addition of sodium ions and then solvated within a truncated octahedron of TIP3P water molecules
208 extending 8 Å from the surface of the protein. Using the Amber 14 molecular dynamics package
209 CUDA version (Salomon-Ferrer et al, 2013; Goetz et al, 2012; Le Grand et al, 2013), the system was
210 energy-minimised for 2,000 cycles using a non-bonded cut-off of 12 Å and then heated under
211 constant volume to 300 K over 25 ps under Langevin dynamics (time step = 1 fs). The heating was
212 continued at 300 K for at least 200 ns under constant pressure also using Langevin dynamics (SHAKE
213 on, time step = 2 fs) using the Particle–Mesh–Ewald (PME) method to treat the long range
214 electrostatic interactions with a 12 Å non-bonded cut-off.

215

216 **Results:**

217 In this paper we have identified that *M. abscessus* can be sensitised to amoxicillin by the addition of
218 the competitive β-lactamase inhibitor, relebactam. Furthermore we have shown that meropenem
219 sensitivity can be enhanced by the addition of relebactam. Firstly, we conducted disk diffusion
220 assays with amoxicillin and meropenem with and without relebactam. Subsequently the zones of
221 inhibition (ZOI) were measured as a marker of sensitivity. Amoxicillin alone failed to demonstrate
222 any kind of sensitivity, however the addition of relebactam provided a clear ZOI, demonstrating the
223 induced sensitivity to amoxicillin by relebactam. A ZOI was visible for meropenem, however with the
224 incorporation of relebactam, this ZOI was significantly enhanced, suggesting increased sensitivity
225 upon combination with relebactam (1a). This led us to the hypothesis that relebactam was inhibiting
226 the *M. abscessus* β-lactamase, Bla_{Mab}, preventing hydrolysis of amoxicillin to the inactive amoxicilloic
227 acid (1b). In order to assess the clinical relevance of these observations, both amoxicillin and
228 meropenem were tested alone and in combination with relebactam against a panel of clinical
229 isolates of *M. abscessus* obtained from patients at Brighton and Sussex Medical School in addition to
230 *M. abscessus* NCTC strain. In all cases, the addition of relebactam sensitised the isolate to amoxicillin
231 (*n=3*) (1c left). The same experiment was conducted with meropenem, and in most cases, an
232 increase in sensitivity was observed (*n=3*) (1c right). All necessary controls were conducted and no
233 ZOI was observed for relebactam alone.

234

235 In order to further validate our observation, liquid cultures were exposed to increasing
236 concentrations of amoxicillin and meropenem with and without a dose response of relebactam (1d
237 top and bottom respectively). As a control, relebactam was also tested for inhibitory activity on its
238 own. These cultures were read every 24 hours using a spectrophotometer at OD_{600nm} up to 96 hours.
239 Relebactam at 128 µg/mL demonstrated no inhibitory activity, giving a growth profile much the
240 same as the compound-free control (no drug), confirming that relebactam lacks antibacterial activity
241 against *M. abscessus*. 32 µg/mL of amoxicillin appeared to show a moderate enhancement of

242 bacterial growth, however when combined with 2 μg/mL of relebactam, this amoxicillin
243 concentration was found to display potent antibacterial activity against *M. abscessus*. The same
244 experiment was conducted with meropenem, wherein partial growth impairment was observed at
245 8 μg/mL, however when combined with 2 μg/mL relebactam, significant antibacterial activity was
246 observed at this concentration. End point statistical analysis was conducted using a t-test to assess
247 the significance of differences between cultures with and without relebactam. In both cases, a
248 statistically significant increase in sensitivity was observed upon addition of 2 μg/mL of relebactam
249 in combination with amoxicillin or meropenem. This experiment was repeated with a Bla_{Mab}
250 overexpressing strain to prove direct binding of relebactam to Bla_{Mab} (1e). The *M. abscessus*
251 containing the Bla_{Mab} constitutive overexpression plasmid pVV16-bla_{Mab} lost sensitivity to the
252 amoxicillin-relebactam combination compared to the empty vector control strain (pVV16-). This
253 result is replicated using the ZOI method (1c), clearly demonstrated drug-target interaction between
254 relebactam and Bla_{Mab}. Plate images and plate map for the subsequent resistance induced by Bla_{Mab}
255 overexpression are shown in Supplementary Figure 1. To briefly explore the wider application for the
256 amoxicillin-relebactam combination against other mycobacterial infections, we tested its activity in
257 liquid culture against the widely used model organism for *Mycobacterium tuberculosis,*
258 *Mycobacterium bovis* BCG (Supplementary Figure 3). Our results show that *M. bovis* BCG amoxicillin
259 sensitivity is enhanced from 200 to 25 μg/mL upon addition of 8 μg/mL relebactam.

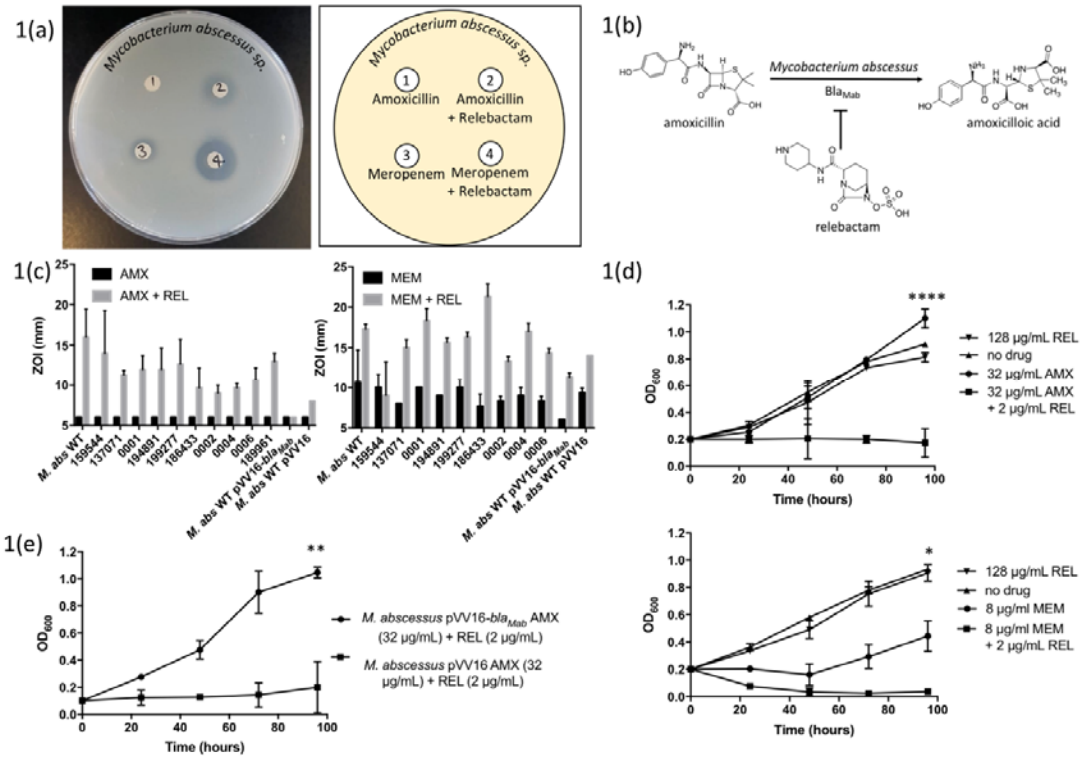

Figure 1: Relebactam sensitises *Mycobacterium abscessus* to amoxicillin and improves sensitivity to meropenem. A disk diffusion experiment (1a) and corresponding plate map demonstrating enhanced sensitivity of *M. abscessus* by zone of inhibition to amoxicillin (1) with the addition of relebactam (2) and meropenem (3) with the addition of relebactam (4). The inhibition of *M. abscessus* -lactamase Bla_{Mab} by relebactam is summarised (1b). The disk diffusion experiments were conducted with the NCTC *M. abscessus* strain along with a panel of clinical isolates and *M. abscessus* pVV16-bla_{Mab} and *M. abscessus* pVV16. The diameter of the zones of inhibition (ZOI) measured in millimetres. All strains of *M. abscessus* tested, except *M. abscessus* pVV16-bla_{Mab}, were resistant to amoxicillin (AMX) alone, however displayed sensitivity with the addition of relebactam (REL). *M. abscessus* pVV16-bla_{Mab} was resistant to amoxicillin both with and without relebactam (1c). The same was conducted for meropenem (MEM) and likewise, activity was clearly enhanced with the addition of relebactam, even in the case of *M. abscessus* pVV16-bla_{Mab} which was resistant to meropenem alone but sensitised with the addition of relebactam (1c). Growth curves were conducted with *M. abscessus* NCTC in medium containing 128 relebactam and 32

275 amoxicillin with and without relebactam at 2 μg/mL. Growth inhibition was only observed with
276 relebactam in combination with amoxicillin (1d). Likewise, the inhibitory activity of meropenem was
277 clearly enhanced with the addition of relebactam (1d). A t-test was used for end point analysis
278 between samples +/- relebactam and the results were deemed to be significant with *p* values of
279 <0.0001 and 0.0152 for amoxicillin and meropenem respectively. The same growth curves were
280 performed with *M. abscessus* pVV16-bla_{Mab} and *M. abscessus* pVV16 in medium containing
281 32 μg/mL amoxicillin with and without relebactam at 2 μg/mL (1e). *M. abscessus* pVV16-bla_{Mab}
282 displayed resistance to amoxicillin and relebactam together whereas *M. abscessus* pVV16 retained
283 sensitivity to amoxicillin and relebactam (p = 0.0017).

284

285 In order to validate the inhibitory activity observed phenotypically in Figure 1, we conducted
286 biochemical analysis of the activity of relebactam on the *M. abscessus* endogenous β-lactamase,
287 Bla_{Mab}. The gene was amplified by PCR, digested, ligated into pET28a and sequenced, before
288 transformation into chemically competent *E. coli* BL21. Bla_{Mab} was expressed, cells harvested and the
289 enzyme purified by IMAC. We subsequently devised a novel TLC-based assay for assessing β-
290 lactamase activity by separating the penicillin V substrate from the penicilloic acid product. This
291 assay enabled us to demonstrate the β-lactamase activity of our purified Bla_{Mab} (2a), as well as assay
292 the efficacy of inhibitors against the enzyme (Supplementary 2a and 2b). We used avibactam as a
293 positive control, as its inhibitory activity against Bla_{Mab} has previously been described by Lefebvre et
294 al. 2017. Lane 1 contained protein purification buffer only, and lane 2 had the addition of enzyme
295 (0.01 mg/mL). Following chromatography, two lower spots are observed in lanes 1 and 2, indicative
296 of buffer. Penicillin V was added to lane 3 and gave a characteristic spot of high R_f value,
297 demonstrating unhydrolysed penicillin resulted in a spot just below the solvent front. Lane 4 was
298 identical to lane 3 with the addition of Bla_{Mab} protein. The hydrolysis of penicillin V to penicilloic acid
299 by Bla_{Mab} resulted in a spot with reduced R_f value. The pre-incubation of enzyme with avibactam in

300 lane 5 resulted in a loss of the lower penicilloic acid spot, demonstrating the inhibition of Bla_{Mab}
301 activity. In lane 6, relebactam alone did not resolve on the TLC, but its pre-incubation with Bla_{Mab}
302 before addition to the penicillin substrate in lane 7 resulted in total inhibition of hydrolysis as
303 observed with avibactam (lane 5). Finally, the inhibition of Bla_{Mab} is further validated by the repeat of
304 lane 4 and lane 7 conditions with heat-denatured Bla_{Mab} (lanes 8 and 9 respectively). This result
305 confirms the direct inhibition of Bla_{Mab} by relebactam (*n=5*).

306

307 We investigated the kinetic parameters of the Michaelis-Menten kinetics, the apparent K_i ($K_{i\ app}$), the
308 second-order carbamylation rate constant (K_2/K_i) and the decarbamylation rate constant (K_{off}) of
309 relebactam inhibition of soluble recombinant Bla_{Mab} using a commercially available β-lactamase
310 substrate, nitrocefin, as a reporter substrate. Nitrocefin is selectively hydrolysed by β-lactamases,
311 resulting in an increase in absorbance which can be monitored at 486 nm. By pre-incubating Bla_{Mab}
312 enzyme with a dose response of relebactam (from 0-100 µM), before initiation of the absorbance
313 assay with the addition of nitrocefin substrate, we observed partial inhibition at 1 µM (0.348 µg/mL)
314 and a complete loss of activity at 10 µM (3.48 µg/mL), confirming the direct inhibitory activity of
315 relebactam on Bla_{Mab} (2b).

316

317 The initial velocities (v_i) of nitrocefin turnover were recorded for a range of nitrocefin concentrations
318 (1-500 µM) over a range of relebactam concentrations (0-2.5 µM). These results were plotted as
319 classical Michaelis-Menten curves (v_i vs [S]) (2c), resulting in Michaelis constants (K_m) between
320 69.43-16.96 µM, before initial velocities were abolished at 2.5 µM relebactam. However, we were
321 unable to derive a K_i value using this data. In response, we plotted the reciprocal initial velocities
322 against relebactam concentrations as a linear equation and derived $K_{i\ app}$ observed from the Y
323 intercept/slope, which was then normalised for the use of nitrocefin (2f) (Papp-Wallace et al., 2018).
324 The $K_{i\ app}$ value obtained of 183.6 nM is indicative of the high inhibitory potency of relebactam

325 against Bla_{Mab}. The carbamylation rate constant (K_2/K_i) of 2.32 x 10^6 $M^{-1}s^{-1}$ is similar to the observed
326 rate for avibactam inhibition of Bla_{Mab} (4.9 x 10^5 $M^{-1}s^{-1}$) (Dubée et al., 2014). The rate of
327 decarbamylation (K_{off}) of Bla_{Mab} for relebactam was 0.0146 min^{-1}, which is again similar to the rate
328 previously obtained for that of avibactam (0.047 min^{-1}) (Dubée et al., 2014). Our kinetics analysis
329 show that, like avibactam, relebactam is a potent, competitive and reversible inhibitor of Bla_{Mab},
330 displaying a reasonably rapid "on" rate and slow "off" rate, with only half the enzyme recovering
331 activity after 40 minutes in the absence of relebactam (2e) (Dubée et al., 2014).

332

333 Our TLC-based β-lactamase assay enabled us to further explore the parameters of the inhibitory
334 activity of relebactam by varying the time of pre-incubation of relebactam with Bla_{Mab}
335 (Supplementary 2a) and the minimum inhibitory concentration required to abrogate catalytic
336 turnover of the penicillin V substrate to the penicilloic acid substrate (Supplementary 2b). We found
337 that penicillin V turnover was rapid and that only addition of relebactam at the same time as the
338 substrate demonstrated turnover of penicillin V, suggesting competitive, reversible inhibition of
339 Bla_{Mab} by relebactam. The dose response of relebactam demonstrated total inhibition down to 20
340 µg/mL, and activity of Bla_{Mab} was maintained below a relebactam concentration of 2 µg/mL. This
341 suggested a minimal concentration of relebactam required to inhibit Bla_{Mab} in the assay is within the
342 range of 20 to 2 µg/mL. This corresponds to a less than or equal to 100 fold stoichiometric excess of
343 relebactam required to completely inhibit Bla_{Mab} (0.5 µM BlaMab to 57.5 µM relebactam
344 corresponding to 20 µg/mL).

2(a)

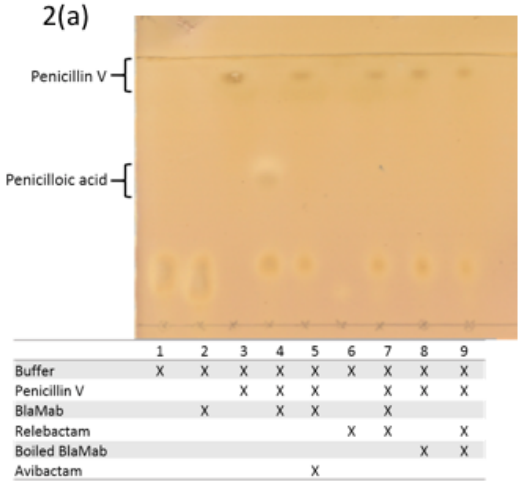

2(b)

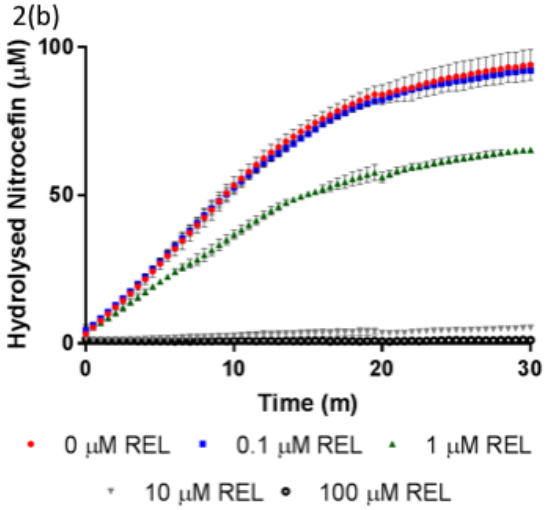

2(c)

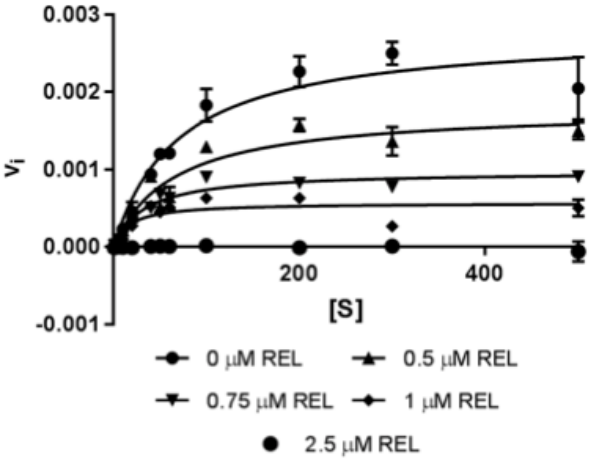

2(d)

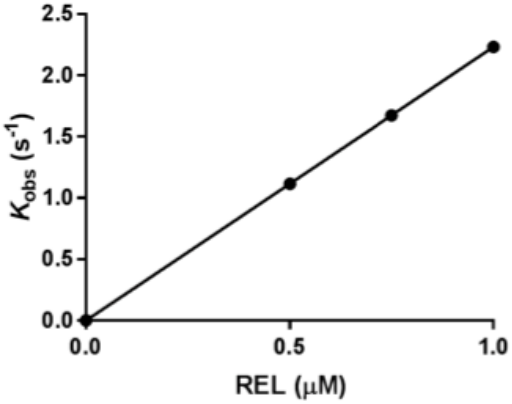

2(e)

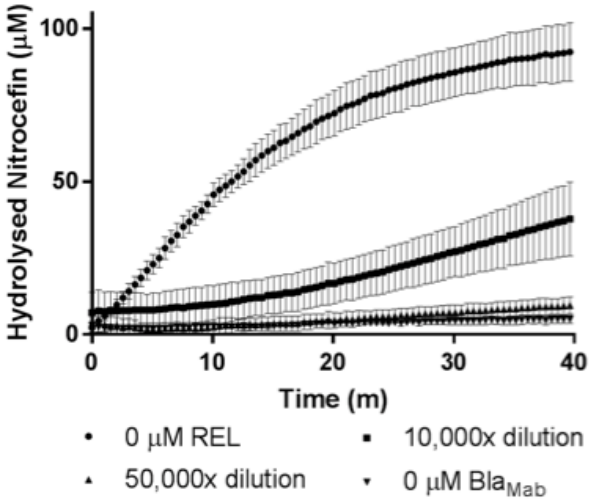

2(f)

Kinetic parameter	Value for Bla_{Mab}
K_m	69.43 μM
$K_{i\ app}$	183.6 nM
K_2/K_i	2.32×10^6 $M^{-1}s^{-1}$
K_{off}	0.0146 min^{-1}

345

346 **Figure 2. Biochemical analysis of relebactam inhibition of *M. abscessus* β-lactamase, Bla_{Mab}.** Our
347 novel Thin Layer Chromatography (TLC) assay (2a) exhibiting the activity of Bla_{Mab} in the turnover of
348 penicillin V (high R_f value) to penicilloic acid (lower R_f value). In the absence, or termination of
349 activity of Bla_{Mab} (by boiling (100 °C) for 1 h) or addition of known inhibitor avibactam (Lefebvre et
350 al., 2017) (200 µg/mL) no lower R_f value spot corresponding to penicilloic acid is seen on the TLC
351 plate. The addition of relebactam to the reaction between Bla_{Mab} and penicillin V also results in the
352 absence of the lower Rf value spot, suggesting inhibition of Bla_{Mab} (2a). This observed inhibition is
353 validated by a spectrophotometric analysis, where the turnover of nitrocefin (100 µM) by Bla_{Mab}
354 (0.25 nM) was monitored at 486 nm with a varying concentration of relebactam (0, 0.1, 1, 10 and
355 100 µM). The increase in concentration of relebactam resulted in partial inhibition of nitrocefin
356 turnover at 1 µM and total abrogation at 10 µM (2b). The initial velocity (v_i) of the reaction between
357 Bla_{Mab} and nitrocefin was monitored for a range of substrate concentrations (1-500 µM) and
358 relebactam concentrations (0, 0.5, 0.75, 1 and 2.5 µM). This data was plotted v_i vs [S] in order to
359 determine K_m values (2c/f). The values for K_{obs} were obtained as previously described (Dubée et al.,
360 2014) and plotted against relebactam concentrations ([I]) to deduce a carbamylation rate (K_2/K_i) for
361 Bla_{Mab} (2d). The kinetics of Bla_{Mab} decarbamylation were assessed to show the recovery of nitrocefin
362 hydrolysis by Bla_{Mab} after inhibition by relebactam in order to derive a K_{off} value (2e). Kinetic
363 parameters were derived as described previously (2f) (Dubée et al., 2014).
364
365

366 In order to further investigate the mechanism of relebactam inhibition of Bla_{Mab}, we conducted
367 molecular docking simulations *in silico*. 6 potential binding sites were identified (3(c)). For pockets 2-
368 6 the ligand was weakly-held and generally exited the pocket after a few tens of nanoseconds. For
369 pocket 1 (corresponding to the main active site) the ligand reoriented itself relative to the docked
370 conformation and thereafter remained relatively stable within the pocket. The binding interactions
371 for the stable pose are shown in Figure 3(a) and 3(b) and include several polar interactions with the
372 sulphonamide moiety and hydrophobic interactions between the relebactam central piperidine ring
373 and tryptophan 106. In addition, after the initial reorientation, the relebactam carbonyl carbon
374 remained in the vicinity of the hydroxyl oxygen of the catalytically-active serine 71 as can be seen
375 after 120 ns in the distance plot given in Figure 3(d). The average distance in this period was
376 approximately 5.5 Å and there were many close approaches. Furthermore, the corresponding O-C=O
377 angle (Figure 3d) in the same period was roughly 130 ° and as such it is reasonable to assume that it
378 would be possible for the serine hydroxyl to attack the relebactam carbonyl and effect a ring-
379 opening. A further molecular dynamics simulation of the enzyme in a periodic box of explicit water
380 was undertaken but this time in the presence of ten copies of unbound relebactam. Over the course
381 of a 200 ns simulation, one ligand found its way into the main active site (pocket 1) after 130 ns and
382 remained stable therein. The other nine copies of the ligand found no place to reside in the enzyme.

383

384

385

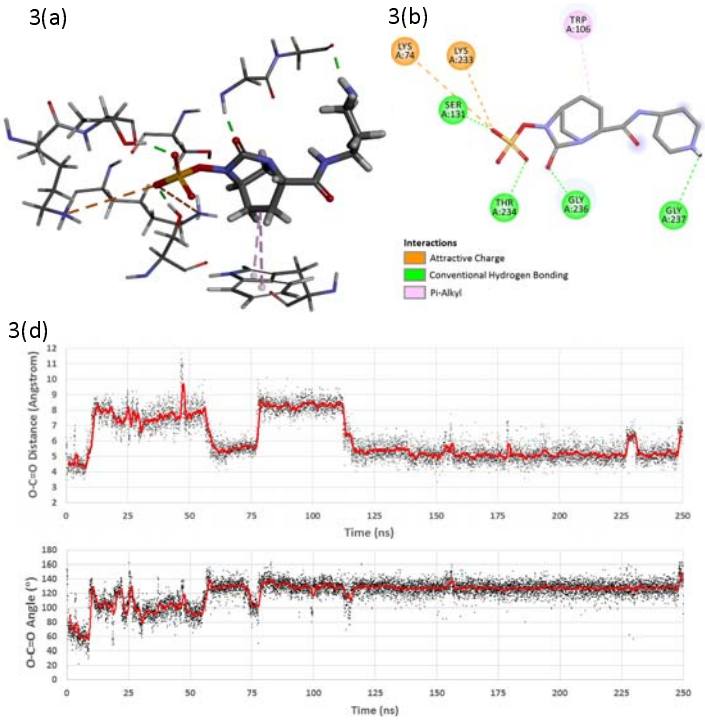

Pocket 1	Pocket 2	Pocket 3	Pocket 4	Pocket 5	Pocket 6
LEU68	ARG45	MET69	PHE76	THR207	ARG95
MET69	GLU65	CYS70	ILE77	ASP208	TYR98
CYS70	ARG66	SER71	VAL78	TRP209	ALA107
SER71	PHE67	THR72	SER79	LEU210	PRO108
TYR72	LEU68	VAL73	ALA80	LYS211	ILE109
VAL73	MET69	LYS74	ILE81	ARG212	THR110
LYS74	CYS70	THR75	LEU82	ASN213	SER111
THR75	ARG165	PHE76	ARG83	THR214	GLN112
PHE76	LEU170	ILE77	ARG84	THR215	HIS113
ILE77	ASN171	VAL78	ARG85	GLY216	GLY117
TRP106	ILE172	ALA80	LEU86	ASP127	MET118
THR127	PRO173	THR127	SER87	GLN218	THR119
LEU128	ASP174	ALA136	GLU88	SER219	VAL120
TYR130	GLY175	ASN137	LEU91	ILE220	SER121
SER131	ASP176	LEU139	GLN142	ARG221	GLU122
ASP132	LEU177	ILE140	LEU143	ALA222	LEU123
ASN133	ASP178	THR141	GLY145	ALA223	CYS124
ALA136	THR179	LEU143	GLY145	VAL224	ASP125
GLU167	SER180	GLY144	LYS147	PRO225	ALA126
VAL168	GLY237	GLY145	GLU148	ALA226	THR127
LEU170	PHE238	PRO146	THR149	GLY227	LEU128
ASN171	LYS239	LYS147	GLU150	TRP228	ARG129
ASP178	GLY240	GLU148	LYS151	THR229	TYR130
LEU210	GLU241	THR149	PHE152	VAL230	ASP132
THR215	THR242	GLU150	VAL153	ALA231	GLY135
LYS233	ASN243	LYS151	ARG154	ASP232	TRP209
THR234	LEU261	VAL153	SER155	LYS233	ARG212
GLY235	THR262	THR161	LEU156	THR234	
GLY236	VAL263	ARG162	GLY197	ASP244	
GLY237	PRO264	MET163	LEU198	ILE245	
ASN243		ASP164		ALA246	
ILE234		ARG165		VAL247	
		THR166		ILE248	
		GLU167		TRP249	
		GLN169		PRO250	
		LEU170		PRO251	
		ASN171		ILE256	
		LEU177		MET258	
		ASP178		ILE276	
		THR179		ALA277	
				THR380	
				ARG281	
				LEU284	
				ALA289	

Figure 3: *In Silico* modelling of the possible interaction of relebactam with the *M. abscessus* β-lactamase, Bla_{Mab}. 3D and 2D protein-ligand interaction diagrams for relebactam in the main (catalytic) active site after molecular dynamics simulation (3a and 3b respectively). Amino acid residues featured in the top six potential binding pockets identified for Bla_{Mab}. Pocket 1 corresponded to the main (catalytic site) in the enzyme and for the purposes of the docking experiment was redefined as all amino acid residues within 8 Å of serine 71 (3c). Time-courses of the serine 71 hydroxyl oxygen – relebactam carbonyl carbon distance and the corresponding O-C=O angle. The actual values are plotted as black points and a 50-frame moving average is over-plotted in red (3d).

Discussion:

In this paper we have demonstrated the inhibitory activity of the non-β-lactam based β-lactamase inhibitor, relebactam against *M. abscessus* endogenous β-lactamase, Bla_{Mab}. Alone, this is not sufficient to kill *M. abscessus,* however its use as part of a combination opens up considerable

401 therapeutic potential. We have identified that a low concentration of relebactam co-administration
402 is capable of sensitising *M. abscessus* NCTC and clinical isolates to amoxicillin, well within the
403 therapeutic range for this versatile and widely available antibiotic. Furthermore, we demonstrate
404 relebactam provides a significant increase in inhibitory activity of meropenem, a mainstay of *M.*
405 *abscessus* clinical intervention. Our study introduces a completely novel TLC-based β-lactamase
406 inhibition assay, validated with the commercially available and widely used nitrocefin assay, to
407 investigate the parameters of relebactam's inhibitory activity. The results of both the kinetics
408 analysis and the *in silico* binding studies demonstrate the mechanism of inhibition of Bla_{Mab} by
409 relebactam as competitive reversible, displaying a reasonably rapid "on" rate and slow "off" rate,
410 indicative of the high potency of the inhibitor against Bla_{Mab}.

411

412 Relebactam is currently in phase III clinical trial for administration in combination with imipenem,
413 another mainstay in *M. abscessus* front line chemotherapy. Our findings therefore represent a
414 timely and highly impactful discovery that is easily translatable into the clinical setting, not only
415 providing a new therapeutic option for *M. abscessus* infections, but with the potential to treat other
416 mycobacterial infectious diseases such as tuberculosis.

417

418 **Author Contributions:**

419 R. C. L., J. H., M. D., D. L. R, P. L. and J. A. G. C. intellectually conceived and designed the experiments.
420 R. C. L., J. H., S. E. R. G, D. L. R. and J. A. G. C. conducted the experiments. R. C. L., J. H., D. L. R. and J.
421 A. G. C. wrote the manuscript.

422

423 **Funding:** This research was funded by Birmingham Women's and Children's Hospital Charity
424 Research Foundation (BWCHCRF) (R. C. L. 50% PhD Studentship, match funded by Aston University

425 Prize Scheme) and the Academy of Medical Sciences and Global Challenges Research Fund with a
426 Springboard Grant (SBF003\1088:).

427

428 **Acknowledgements:** J. A. G. C. is grateful to the Academy of Medical Sciences, Global Challenges
429 Research Fund and Birmingham Women's and Children's Hospital Charity Research Foundation
430 (BWCHCRF) for their continued support of the Mycobacterial Research Group at Aston University.
431 The *Mycobacterium abscessus* clinical isolates used in this study were provided by Dr Simon
432 Waddell, Brighton and Sussex Medical School. We are also grateful to Dr Amit Chattopadhyay, Aston
433 University, for technical support.

434

435 **References:**

436 Bryant, J. M., Grogono, D. M., Greaves, D., Foweraker, J., Roddick, I., Inns, T., Reacher, M., Haworth,
437 C. S., Curran, M. D., Harris, S. R., Peacock, S. J., Parkhill, J., Floto, R. A. (2013) Whole-genome
438 sequencing to identify transmission of Mycobacterium abscessus between patients with cystic
439 fibrosis: a retrospective cohort study. *Lancet,* 381, 1551-1560

440 Case, D. A., Cheatham, T. E., Darden, T., Gohlke, H., Luo, R., Merz, K. M., Onufriev, A., Simmerling,
441 C., Wang, B., Woods, R. J., (2005) The Amber biomolecular simulation programs. *Journal of*
442 *Computational Chemistry*, 26, 1668-1688.

443 Dubée, V., Bernut, A., Cortes, M., Lesne, T., Dorchene, D., Lefebvre, A., Hugonnet, J., Gutmann, L.,
444 Mainardi, J., Herrmann, J., Gaillard, J., Kremer, L., Arthur, M., (2014) β-Lactamase inhibition by
445 avibactam in Mycobacterium abscessus, Journal of Antimicrobial Chemotherapy, 70 (4), 1051–1058.

446 Fitzgerald, D. A., Smith, A. G., Lees, A., Yee, L., Cooper, N., Harris, S.C., Gibson, J. A. (1995) Cutaneous
447 infection with Mycobacterium abscessus. *British Journal of Dermatology*. 132. 800-804.

448 Goetz, A. W., Williamson, M. J., Xu, D., Poole, D., Le Grand, S., Walker, R. C., (2012) Routine
449 microsecond molecular dynamics simulations with AMBER on GPUs. 1. Generalized born. *Journal*
450 *of Chemical Theory and Computation*, 8, 1542-1555.
451 Griffith, D. E., Aksamit, T., Brown-Elliott, B. A., Catanzaro, A., Daley, C., Gordin, F., Holland, S. M.,
452 Horsburgh, R., Huitt, G., Iademarco, M. F., Iseman, M., Olivier, K., Ruoss, S., von Reyn, C. F., Wallace,
453 R. J., Winthrop, K. (2007) An Official ATS/IDSA Statement: Diagnosis, Treatment, and Prevention of
454 Nontuberculous Mycobacterial Diseases. *American Journal of Respiratory Critical Care Medicine*.
455 175, 367-416

456 Griffith, D.E. (2014) *Mycobacterium abscessus* subsp *abscessus* lung disease: 'trouble ahead, trouble
457 behind…'. *F1000Prime Reports.* 6, 1-6

458 Haworth, C. S., Banks, J., Capstick, T., Fisher, A. J., Gorsuch, T., Laurenson, I. F., Leitch, A., Loebinger,
459 M. R., Milburn, H. J., Nightingale, M., Ormerod, P., Singhadia, D., Smith, D., Whitehead, N., Wilson,
460 R., Floto, R. A. (2017) British Thoracic Society guidelines for the management of non-tuberculous
461 mycobacterial pulmonary disease (NTM-PD). *Thorax*, 72, 1-64

462 Caleffi-Ferracioli, K.R., Maltempe, F. G., Siqueira, V. L. D., Cardoso, R. F., (2013) Fast detection of
463 drug interaction in *Mycobacterium tuberculosis* by a checkerboard resazurin method, Tuberculosis,
464 Volume 93, Issue 6, Pages 660-663, ISSN 1472-9792, https://doi.org/10.1016/j.tube.2013.09.001.

465 Kaushik, A., Ammerman, N. C., Lee, J., Martins, O., Kreiswirth, B. N., Lamichhane, G., Parrish, N. M.,
466 Nuermberger, E. L. (2019) *In Vitro* Activity of the New β-Lactamase Inhibitors Relebactam and
467 Vaborbactam in Combination with β-Lactams against Mycobacterium abscessus Complex Clinical
468 Isolates. *Antimicrobial Agents and Chemotherapy,* 63, 1-11

469 Kawabata, T., Go, N., (2007) Detection of pockets on protein surfaces using small and large probe
470 spheres to find putative ligand binding sites. *Proteins*, 68,516-529.

471 Kawabata, T., (2010) Detection of multi-scale pockets on protein surfaces using mathematical
472 morphology. *Proteins*, 78, 1195-1121.

473 Kehrmann, J., Kurt, N., Rueger, K., Bange, F.C., Buer, J., (2016) GenoType NTM- DR for identifying
474 *Mycobacterium abscessus* subspecies and determining molecular resistance. J Clin Microbiol
475 54:1653–1655. doi:10.1128/JCM.00147-16.

476 Le Grand, S., Goetz, A. W., Walker, R. C. (2013) SPFP: Speed without compromise - a mixed
477 precision model for GPU accelerated molecular dynamics simulations. *Computer Physics*
478 *Communications*, 184, 374-380.

479 Lefebvre A-L, Le Moigne V, Bernut A, Veckerlé C, Compain F, Herrmann J-L, Kremer L, Arthur M,
480 Mainardi J-L. 2017. Inhibition of the β-lactamase Bla by avibactam improves the *in vitro* and *in vivo*
481 efficacy of imipenem against *Mycobacterium abscessus*. Antimicrob Agents Chemother 61:e02440-
482 16. https://doi.org/ 10.1128/AAC.02440-16.

483 Leung, J., and Olivier, K. 2013. Nontuberculous mycobacteria in patients with cystic fibrosis. *Semin*
484 *Respir Crit Care Med.* 34(1):124

485 Lopeman, R.C.; Harrison, J.; Desai, M.; Cox, J.A.G. *Mycobacterium abscessus:* Environmental
486 Bacterium Turned Clinical Nightmare. *Preprints* 2019, 2019010273 (doi:
487 10.20944/preprints201901.0273.v1).

488 Moore, M and Frerichs, JB. 1953. *An Unusual Acid-Fast Infection of the Knee with Subcutaneous,*
489 *Abscess-Like Lesions of the Gluteal Region. 2*, Journal of Investigative Dermatology, Vol. 20.

490 Nessar R, Cambau E, Reyrat JM, Murray A, Gicquel B. 2012. Mycobacterium abscessus: a new
491 antibiotic nightmare. J Antimicrob Chemother 67:810–818. https://doi.org/10.1093/jac/dkr578.

492 Pandey R, Chen L, Manca C, Jenkins S, Glaser L, Vinnard C, Stone G, Lee J, Mathema B, Nuermberger
493 EL, Bonomo RA, Kreiswirth BN. 2019. Dual β-lactam combinations highly active against
494 *Mycobacterium abscessus* complex *in vitro*. mBio 10:e02895-18. https://
495 doi.org/10.1128/mBio.02895-18.

496 Papp-Wallace, K. M., Barnes, M. D., Alsop, J., Taracila, M. A., Bethel, C. R., Becka, S. A., van Duin,
497 D., Kreiswirth, B. N., Kaye, K. S., Bonomo, R. A., (2018) Relebactam Is a Potent Inhibitor of the KPC-2
498 β-Lactamase and Restores Imipenem Susceptibility in KPC-Producing *Enterobacteriaceae*
499 Antimicrobial Agents and Chemotherapy, 62 (6) e00174-18.

500 Petrini B. 2006. Mycobacterium abscessus: an emerging rapid-growing potential pathogen. APMIS
501 114:319 –328. https://doi.org/10.1111/j.1600 -0463.2006.apm_390.x.

502 Salomon-Ferrer, R., Goetz, A. W., Poole, D., Le Grand, S., Walker, R. C., (2013) Routine
503 microsecond molecular dynamics simulations with AMBER - Part II: Particle Mesh Ewald. *Journal*
504 *of Chemical Theory and Computation*, 9, 3878-3888.

505 Soni, I., De Groote, M., Dasgupta, A., and Chopra, S. 2016. Challenges facing the drug discovery
506 pipeline for non-tuberculous mycobacteria. *J Med Microbiol.* 65(1):1-8

507 Soroka D, Dubee V, Soulier-Escrihuela O, Cuinet G, Hugonnet JE, Gut- mann L, Mainardi JL, Arthur M.
508 2014. Characterization of broad-spectrum Mycobacterium abscessus class A beta-lactamase. J
509 Antimicrob Che- mother 69:691–696. https://doi.org/10.1093/jac/dkt410.

510 Story-Roller, E., Maggioncalda, E. C., Lamichhane, G. (2019) Select β-Lactam Combinations Exhibit
511 Synergy against *Mycobacterium abscessus In Vitro*. *Antimicrobial Agents and Chemotherapy.* 63, 1-
512 11

513 Tortoli, E, Kohl, TA and Brown-Elliot, BA. 2016. *Emended description of Mycobacterium abscessus,*
514 *Mycobacterium abscessus subsp. abscessus and Mycobacterium abscessus subsp. bolletii and*

515 *designation of Mycobacterium abscessus subsp. massiliense comb. nov*, International Journal of
516 Systematic and Evolutionary Microbiology, Vol. 66, pp. 4471-4479.

517 Wayne, P. A. (2015) Methods for Dilution Antimicrobial Susceptibility Tests for Bacteria That Grow
518 Aerobically; Approved Standard – Tenth Edition. *CLSI document M07-A10.* 32.

1(a)

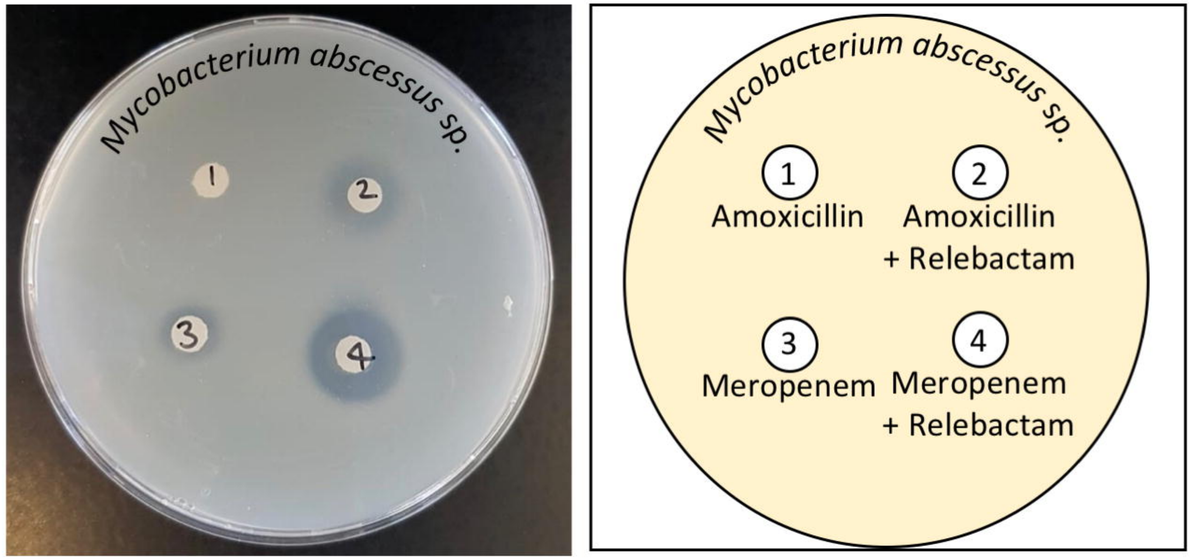
Mycobacterium abscessus sp.
1
2
3
4
Mycobacterium abscessus sp.
1 Amoxicillin
2 Amoxicillin + Relebactam
3 Meropenem
4 Meropenem + Relebactam

1(b)

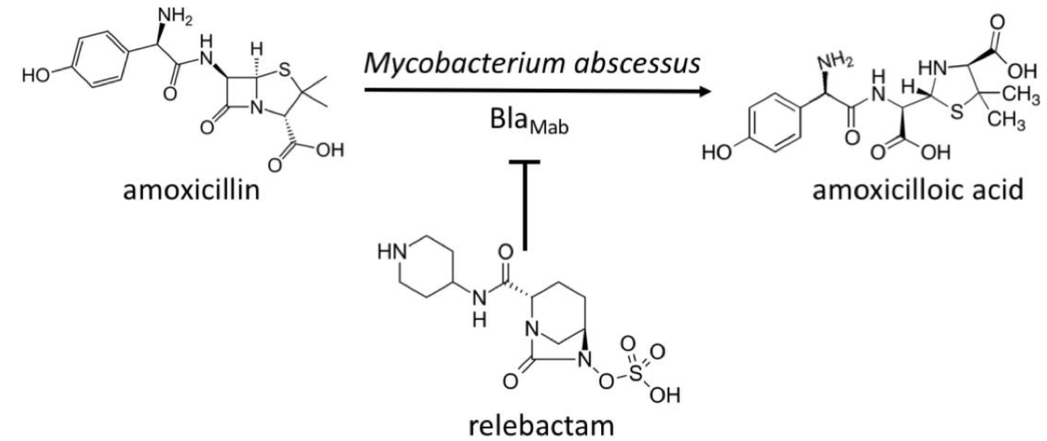
amoxicillin
Mycobacterium abscessus
Bla$_{Mab}$
amoxicilloic acid
relebactam

1(c)

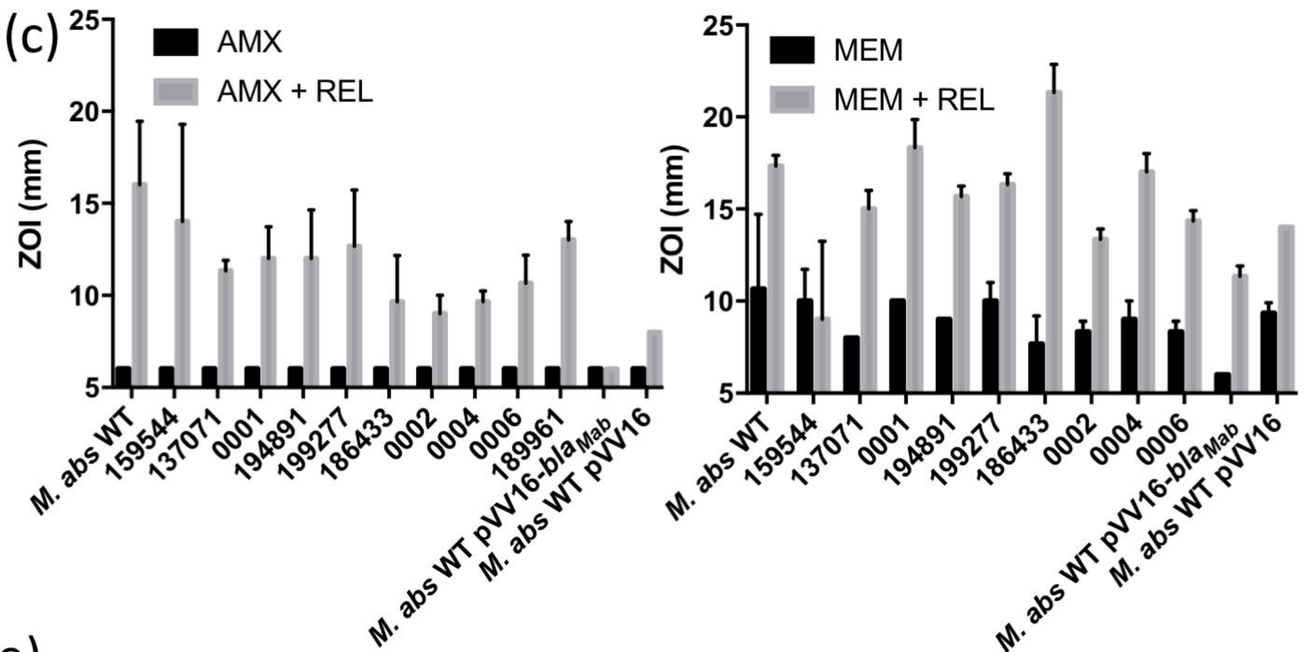
AMX
AMX + REL
ZOI (mm)
M. abs WT
159544
137071
0001
194891
199277
186433
0002
0004
0006
189961
M. abs WT pVV16-bla$_{Mab}$
M. abs WT pVV16
MEM
MEM + REL

1(d)

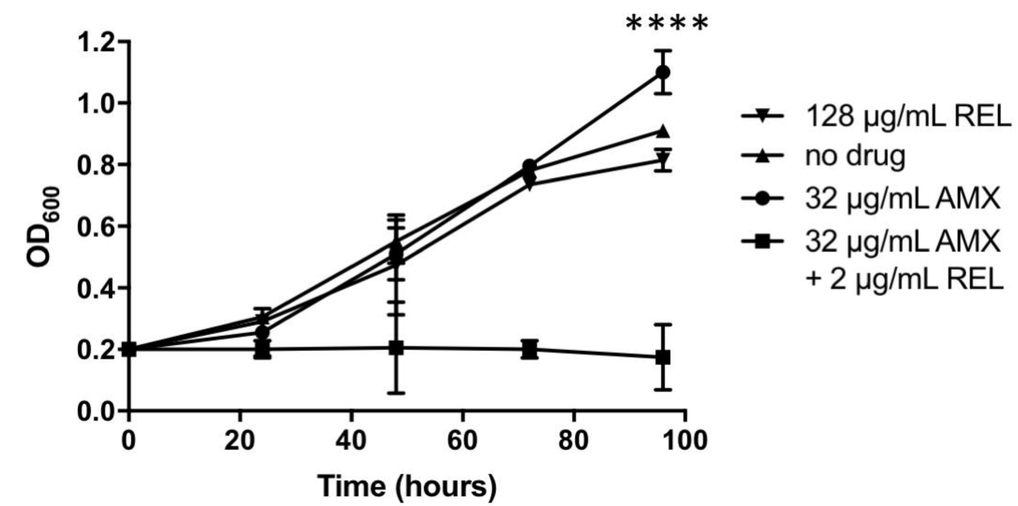
****
OD$_{600}$
Time (hours)
128 µg/mL REL
no drug
32 µg/mL AMX
32 µg/mL AMX + 2 µg/mL REL

1(e)

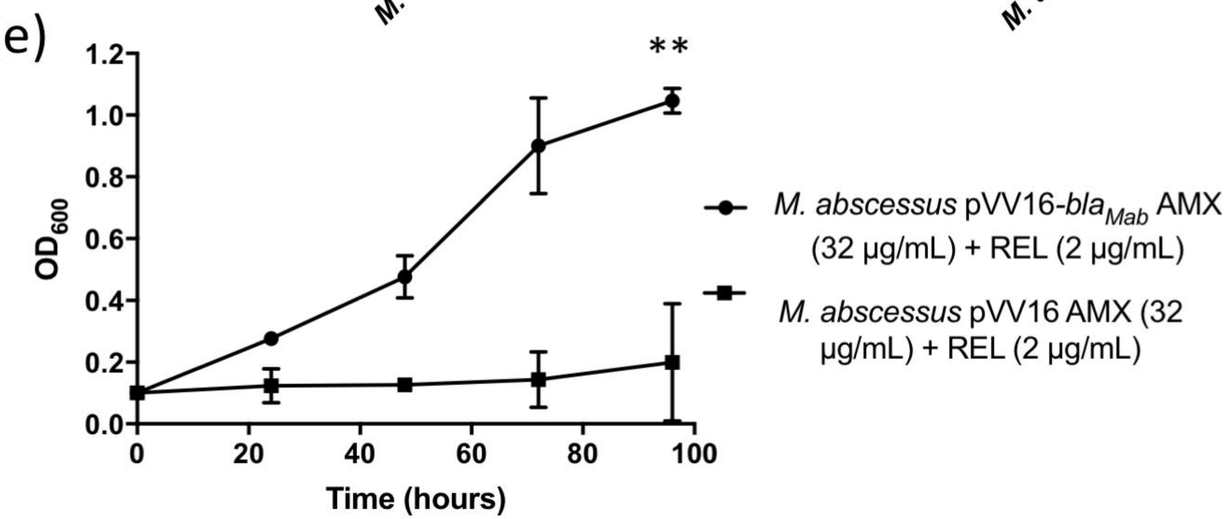
**
OD$_{600}$
Time (hours)
M. abscessus pVV16-bla$_{Mab}$ AMX (32 µg/mL) + REL (2 µg/mL)
M. abscessus pVV16 AMX (32 µg/mL) + REL (2 µg/mL)

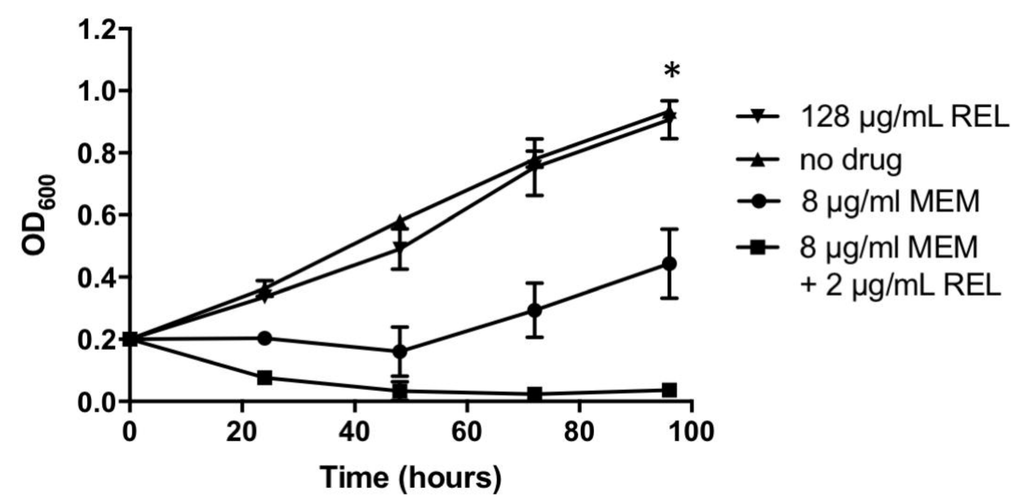
*
OD$_{600}$
Time (hours)
128 µg/mL REL
no drug
8 µg/ml MEM
8 µg/ml MEM + 2 µg/mL REL

2(a)

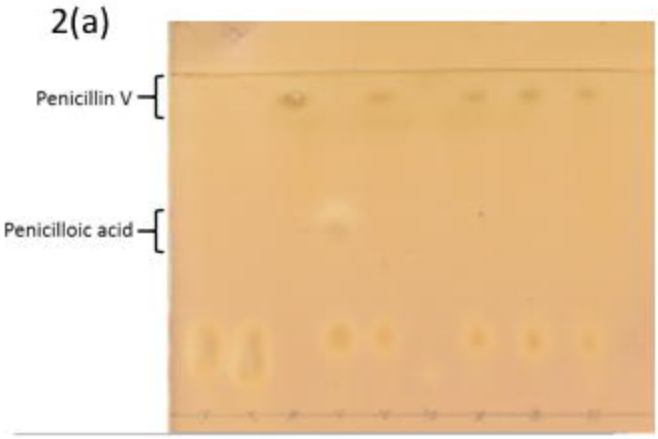

	1	2	3	4	5	6	7	8	9
Buffer	X	X	X	X	X	X	X	X	X
Penicillin V			X	X	X		X	X	X
BlaMab		X		X	X		X		
Relebactam						X	X		X
Boiled BlaMab								X	X
Avibactam					X				

2(b)

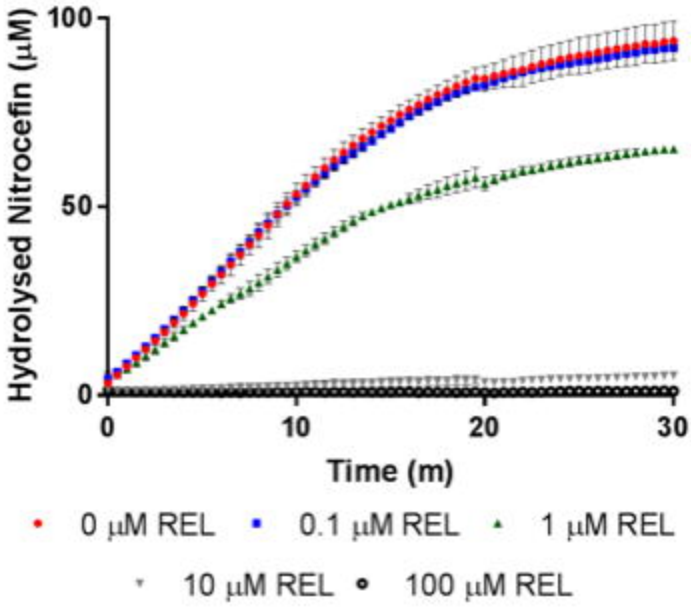

2(c)

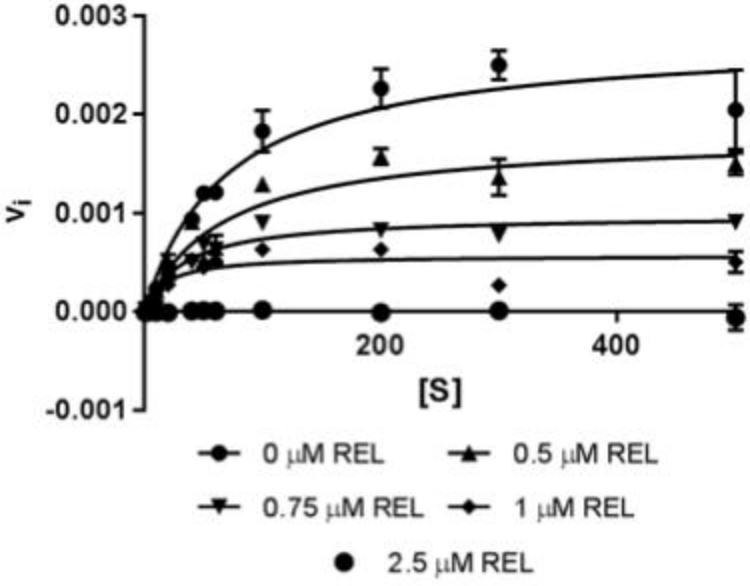

2(d)

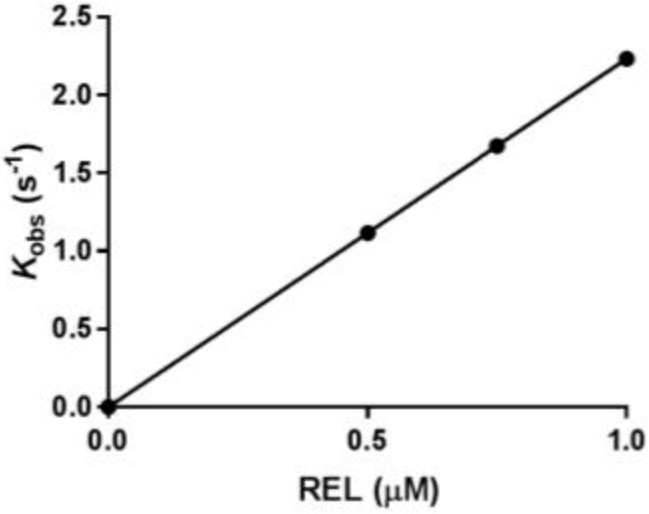

2(e)

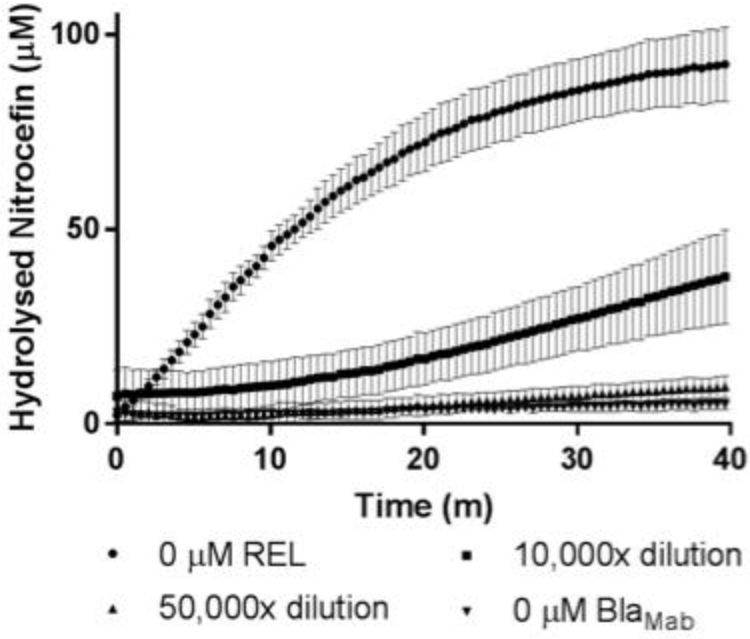

2(f)

Kinetic parameter	Value for Bla_{Mab}
K_m	69.43 μM
$K_{i\ app}$	183.6 nM
K_2/K_i	2.32×10^6 $M^{-1}s^{-1}$
K_{off}	0.0146 min^{-1}

3(a)

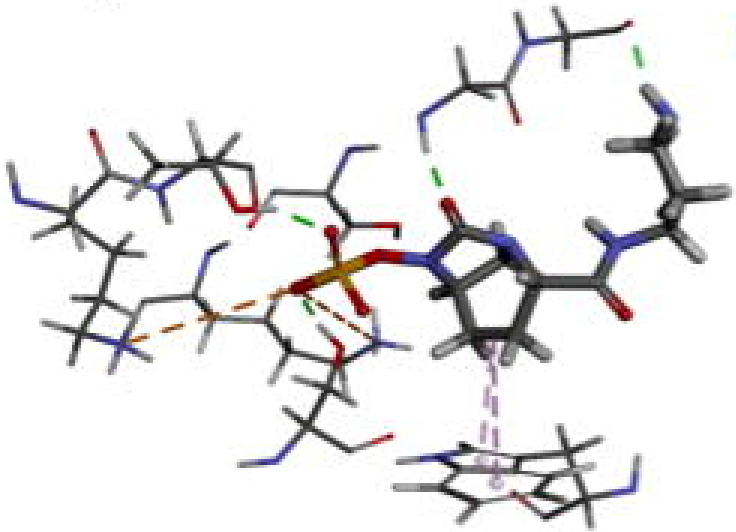

3(b)

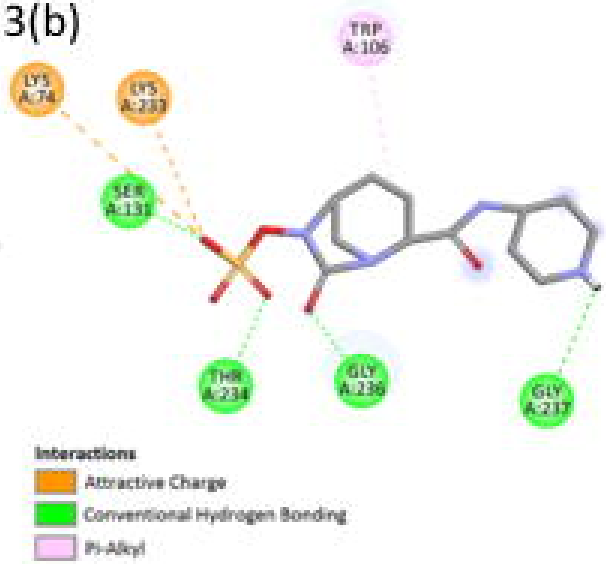

3(c)

Pocket 1	Pocket 2	Pocket 3	Pocket 4	Pocket 5	Pocket 6
LEU68	ARG45	MET69	PHE76	THR207	ARG95
MET69	GLU65	CYS70	ILE77	ASP208	TYR98
CYS70	ARG66	SER71	VAL78	TRP209	ALA107
SER71	PHE67	THR72	SER79	LEU210	PRO108
TYR72	LEU68	VAL73	ALA80	LYS211	ILE109
VAL73	MET69	LYS74	ILE81	ARG212	THR110
LYS74	CYS70	THR75	LEU82	ASN213	SER111
THR75	ARG165	PHE76	ARG83	THR214	GLN112
PHE76	LEU170	ILE77	ARG84	THR215	HIS113
ILE77	ASN171	VAL78	ARG85	GLY216	GLY117
TRP106	ILE172	ALA80	LEU86	ASP127	MET118
THR127	PRO173	THR127	SER87	GLN218	THR119
LEU128	ASP174	ALA136	GLU88	SER219	VAL120
TYR130	GLY175	ASN137	LEU91	ILE220	SER121
SER131	ASP176	LEU139	GLN142	ARG221	GLU122
ASP132	LEU177	ILE140	LEU143	ALA222	LEU123
ASN133	ASP178	THR141	GLY145	ALA223	CYS124
ALA136	THR179	LEU143	GLY145	VAL224	ASP125
GLU167	SER180	GLY144	LYS147	PRO225	ALA126
VAL168	GLY237	GLY145	GLU148	ALA226	THR127
LEU170	PHE238	PRO146	THR149	GLY227	LEU128
ASN171	LYS239	LYS147	GLU150	TRP228	ARG129
ASP178	GLY240	GLU148	LYS151	THR229	TYR130
LEU210	GLU241	THR149	PHE152	VAL230	ASP132
THR215	THR242	GLU150	VAL153	ALA231	GLY135
LYS233	ASN243	LYS151	ARG154	ASP232	TRP209
THR234	LEU261	VAL153	SER155	LYS233	ARG212
GLY235	THR262	THR161	LEU156	THR234	
GLY236	VAL263	ARG162	GLY197	ASP244	
GLY237	PRO264	MET163	LEU198	ILE245	
ASN243		ASP164		ALA246	
ILE234		ARG165		VAL247	
		THR166		ILE248	
		GLU167		TRP249	
		GLN169		PRO250	
		LEU170		PRO251	
		ASN171		ILE256	
		LEU177		MET258	
		ASP178		ILE276	
		THR179		ALA277	
				THR280	
				ARG281	
				LEU284	
				ALA289	
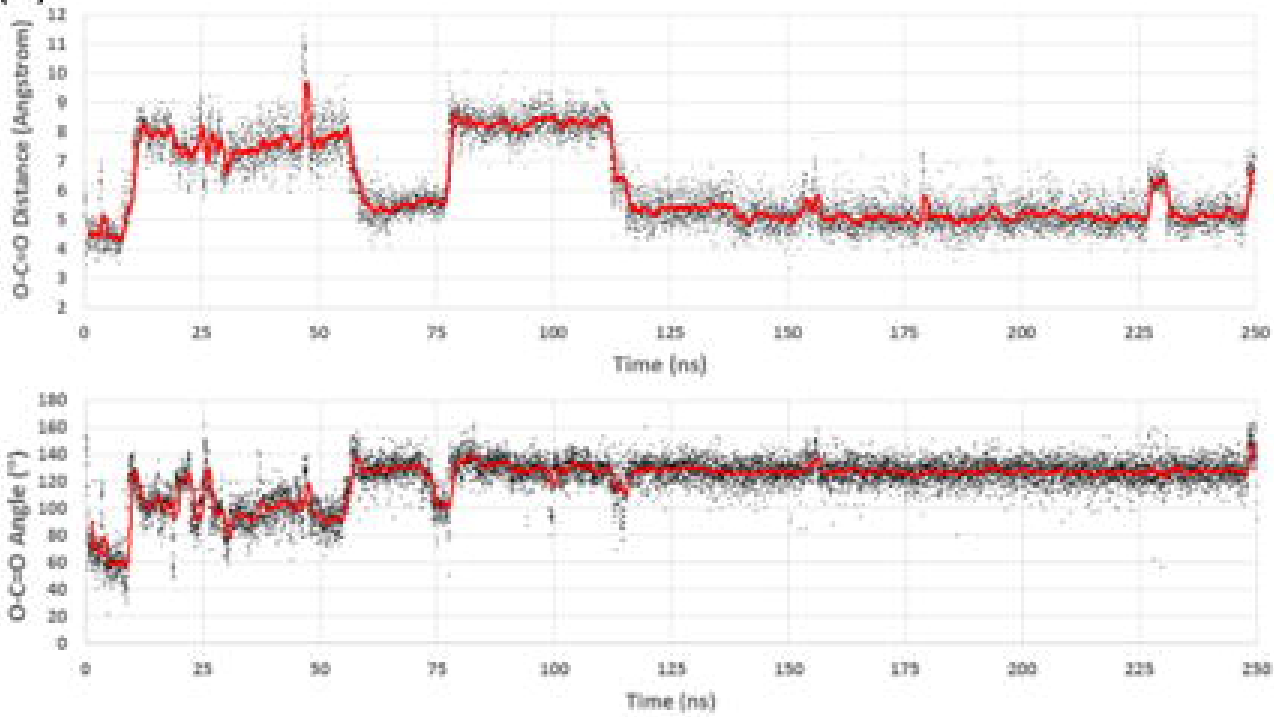
3(d)